Effects of the DNA-Damaging Enediyne C-1027 on Intracellular SV40 and Genomic DNA in Green Monkey Kidney BSC-1 Cells†

Mary M. McHugh,‡ Jan M. Woynarowski,‡,§ Loretta S. Gawron,‡ Toshio Otani,|| and Terry A. Beerman*,‡

Department of Experimental Therapeutics, Roswell Park Cancer Institute, Elm and Carlton Streets, Buffalo, New York 14263, and Tokushima Research Center, Taiho Pharmaceutical Co., Ltd., Kawauchi-cho, Tokushima 771-01, Japan

Received August 24, 1994; Revised Manuscript Received November 9, 1994⊗

ABSTRACT: This study describes the selective ability of C-1027 to induce limited double-strand damage in a viral DNA target. The effect of the cellular environment on C-1027 activity was examined by assaying the extent, as well as the specificity, of damage to simian virus 40 (SV40) DNA in lytically infected mammalian BSC-1 cells and in purified SV40 DNA preparations. C-1027 damage to intracellular SV40 DNA was quantitated by topological forms conversion analysis. A gradual decrease in intracellular supercoiled form I accompanied by an increase in form III was observed with C-1027 concentrations from 2 to 100 nM, with a 50% reduction in form I observed at 50 nM. Damage to purified SV40 DNA also was most pronounced between 10 and 100 nM C-1027. When concentrations were expressed as r values (drug/DNA molar ratio), the amount of C-1027 necessary to effect a 50% reduction in form I was lower for intracellular ($r = 0.002$) than for purified SV40 DNA ($r = 0.0035$). Double-strand damage was more likely to occur with C-1027 treatment of intracellular compared to purified SV40 DNA. However, with both purified and intracellular DNA, restriction enzyme digestion analysis revealed double-strand damage at a number of specific sites throughout the genome, particularly within the early region of the SV40 genome (e.g., within the coding sequence for large T-antigen). No significant damage was observed in either the origin (ORI) or the termination (TER) regions of SV40 replication. The extent of C-1027 damage to uninfected BSC-1 cell DNA was also quantitated using pulsed-field gel electrophoresis. At 0.1 nM ($r = 2.8 \times 10^{-5}$), where incorporation of [^{3}H]thymidine was reduced by 80%, 600 rad equiv of damage was detected in uninfected BSC-1 cells. At C-1027 r values from 1×10^{-4} to 40×10^{-4}, double-strand breaks were from 80- to 40-fold more frequent in SV40 than in BSC-1 cell genomic DNA. By contrast, 50-fold more drug was necessary to inhibit intracellular SV40 DNA accumulation compared to [^{3}H]thymidine incorporation into uninfected BSC-1 cells. Thus, SV40 DNA synthesis appeared to be less sensitive to C-1027-induced lesions than replication in uninfected BSC-1 cells.

Enediyne drugs are a novel group of DNA-damaging antibiotics that have generated much interest in recent years because of their pronounced cytotoxicity and potential antitumor activity (Nicolaou et al., 1993a). In general, naturally occurring enediynes consist of three components: a system to deliver the drug to its DNA target, a DNA-damaging component (i.e., an enediyne-containing chromophore), and a trigger to initiate the series of reactions culminating in DNA damage (Nicolaou et al., 1992). Typically, the DNA-damaging enediyne chromophore binds noncovalently to the minor groove (Nicolaou et al., 1993a). Under the appropriate conditions (e.g., in the presence of thiols), the enediyne is triggered to undergo the Masamune−Bergman reaction to generate a benzenoid diradical, which reacts with DNA. In addition to rapid DNA damage, the cytotoxicity of certain enediyne structures has been attributed to drug-induced cell death or apoptosis (Nicolaou et al., 1993a).

The enediyne, C-1027, is an extremely cytotoxic antitumor antibiotic isolated from *Streptomyces globisporus* (Hu et al., 1988), which displays potent antimicrobial activity against most Gram-positive bacteria and against some strains of Gram-negative bacteria, as well as cytotoxicity against human KB carcinoma cells in culture and certain murine tumors *in vivo* [e.g., L1210, P388, ascites hepatoma H22, sarcoma 180, and melanoma Harding-Passey (Zhen et al., 1989)]. Recent studies have reported that the cytotoxicity of C-1027 is directly dependent on its ability to react with DNA, effecting double- and single-strand damage at AT-rich sites (Sugiura & Matsumoto, 1993; Xu et al., 1994). C-1027 consists of a DNA reactive enediyne-containing chromophore noncovalently bound to an acidic protein molecule (MW 10 500) (Sugiura & Matsumoto, 1993). The structure of the C-1027 chromophore is similar to that of neocarzinostatin (see Figure 1), a well-characterized DNA-damaging antibiotic [for a review, see Goldberg et al (1981)] also classified as an enediyne agent (Myers et al., 1988). While the C-1027 apoprotein has no effect on either site specificity or DNA cleavage (Matsumoto et al., 1993), it serves to stabilize the chromophore activity. In addition, aminopeptidase activity has been associated with the intact holoantibiotic. (Sakata et al., 1992). Such activity may permit easier access of the chromophore component to DNA by facilitating its passage across the cell membrane.

† This study was supported in part by grants from the National Cancer Institute (CA 28495 and CA 16056).

* Author to whom correspondence should be addressed. Telephone: 716-845-3443. Fax: 716-845-8857.

‡ Roswell Park Cancer Institute.

§ Present address: Institute for Drug Development, Cancer Therapy and Research Center, San Antonio, TX 78245.

|| Taiho Pharmaceutical Co., Ltd.

⊗ Abstract published in *Advance ACS Abstracts,* January 15, 1995.

0006-2960/95/0434-1805$09.00/0 © 1995 American Chemical Society

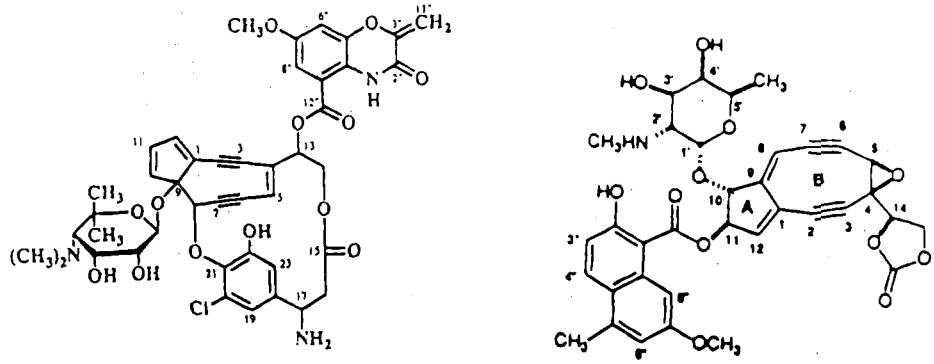

C-1027 Neocarzinostatin

FIGURE 1: Chemical structures of the chromophore components of C-1027 and neocarzinostatin.

Novel aspects of the activity of C-1027 relative to other enediynes include its extreme cytotoxicity [C-1027 is at least 1000-fold more potent than neocarzinostatin (Zhen et al., 1989)] and the fact that thiols are not required for activation (Sugimoto et al., 1990). Rather, C-1027 activity is temperature-dependent, undergoing the Masamune−Bergman reaction at room temperature (Sugiura & Matsumoto, 1993). C-1027-induced strand damage occurs when the cyclized enediyne abstracts hydrogen from the deoxyribose backbone of DNA. A double-strand break results from two single-strand breaks on opposite strands separated by two base pairs (Sugiura & Matsumoto, 1993; Xu et al., 1994).

While C-1027 has been characterized with respect to its structure, chemistry of interaction with isolated DNA, and cytotoxic potency, little is known about its intracellular DNA reactivity. For example, C-1027 was reported by others to induce damage to purified pBR322 DNA at sites such as those containing the sequence 5′-TAT/3′-ATA (Sugiura & Matsumoto, 1993; Xu et al., 1994). If this site preference is extrapolated to intracellular eukaryotic DNA, one would expect a large number of nearly random cleavage sites distributed throughout the genome. However, the high cytotoxicity observed at very low drug dose suggests that a more specific type of damage might be responsible for lethality. Since C-1027 reportedly inhibits DNA synthesis (Sugimoto et al., 1990), one might predict DNA damage to be directed at sequences important for DNA replication. Factors that may limit C-1027 access to DNA and, hence, DNA site preference in eukaryotic cells include the compacting of DNA in the nucleus and its association with chromatin proteins.

Monkey BSC-1 cells in culture are useful for the study of intracellular DNA damage since they provide a mammalian DNA target and can also serve as host for lytic infection with simian virus 40 (SV40) (Tooze, 1980). Drug-induced damage to SV40 DNA in infected cells is readily determined by topological forms conversion analysis [e.g., the loss of supercoiled form I, accompanied by increases in form II (nicked circular) and form III (linear) DNA] and may be mapped to specific regions of the SV40 genome (Tooze, 1980). In uninfected cells, drug levels that damage DNA may be directly compared to those at which cytotoxicity is observed. Finally, drug effects on DNA synthesis may be quantitated in both infected and uninfected cells.

This study describes the selective ability of C-1027 to induce limited single- and double-strand damage to a viral DNA target. The effect of the cellular environment on C-1027 activity was examined by assaying the extent, as well as the specificity, of damage to SV40 DNA in lytically infected mammalian BSC-1 cells and in purified SV40 DNA preparations. DNA damage induction and inhibition of DNA synthesis were compared in C-1027-treated uninfected and SV40-infected BSC-1 cells. Cell growth inhibition was also assayed by quantitating the effects of C-1027 on colony formation by uninfected BSC-1 cells.

EXPERIMENTAL PROCEDURES

Chemicals. C-1027 is produced by the Taiho Co. (Tokyo, Japan). Stock solutions in water were stored at −20 °C. SV40 DNA was purchased from Gibco-BRL (Grand Island, NY) and was diluted in sterile water just before use. [^{32}P]-dCTP was obtained from Dupont NEN (Boston, MA). [*methyl*-^{3}H]Thymidine (48 Ci/mmol) was from CEA (France). [2-^{14}C]Thymidine (56 mCi/mmol, 0.25 mCi/2.5 mL) was purchased from Moravek Biochemical, Inc. (Brea, CA). T7 QuickPrime oligonucleotide labeling kit was from Pharmacia (Milwaukee, WI). *Bgl*I and proteinase K were from Boehringer Mannheim (Indianapolis, IN). Hybond-N nylon membranes were from Amersham (Arlington Heights, IL). Incert agarose was from FMC (Rockland, ME). All other chemicals were of reagent grade.

Cell Culture and Viral Infection. Maintenance of BSC-1 (African green monkey kidney) cells was in Minimal Essential Medium plus 10% calf serum (MEM), and infection with 5−15 plaque-forming units of SV40 virus per 0.6 × 10^6 cells was as described elsewhere (Grimwade et al., 1987).

C-1027 Treatment of SV40 DNA. C-1027 treatment of SV40 DNA routinely was performed as follows. BSC-1 cells (6 × 10^5 per 35 mm plate) were infected as described above with SV40 virus. Forty hours after infection, the plates were rinsed once and incubated for 30 min with fresh medium. Cells were treated for 2 h with C-1027 in 1.0 mL of medium (total volume) and then rinsed once with phosphate-buffered saline (PBS). Purified SV40 DNA (100 ng) was incubated at 37 °C for 15 min with C-1027 in 0.025 mL (final volume) of Tris-HCl (pH 7.6). Reactions with both purified and intracellular DNA routinely were terminated by adjusting samples to a final concentration of 1% sodium dodecyl sulfate (SDS). Proteinase K (50 μg/mL) was added to intracellular samples, which were digested for an additional 2 h. All samples were then extracted with phenol/chloroform/isoamyl alcohol (25:24:1), precipitated with ethanol, and resuspended in TE [10 mM Tris-HCl (pH 8.0) and 1 mM ethylenediaminetetraacetic acid (EDTA)].

Topological Forms Conversion and Restriction Enzyme Digestion Analysis of C-1027 Strand Damage to SV40 DNA. At least three samples per C-1027 concentration were analyzed for damage to both intracellular and purified SV40 DNA. Samples were prepared as described above and divided into two aliquots. One aliquot was subjected to digestion with the single-cut restriction enzyme *BglI*. The other aliquot was not restricted. Both nonrestricted and restricted samples were electrophoresed on 1% agarose gels in TAE for 20 h at 1.5 V/cm. Gels containing nonrestricted samples were stained with ethidium bromide (0.5 μg/mL), and the SV40 DNA was visualized and photographed over an ultraviolet light source using a Polaroid CU-5 land camera. Gels containing restricted samples were blotted to nylon membranes and hybridized to the *TaqI*−*BglI* fragment of SV40 DNA. This fragment was radiolabeled with α-^{32}P using the T7 QuickPrime oligonucleotide labeling kit. Blotting, hybridization, and autoradiography of the blots were performed as described elsewhere (Sambrook et al., 1989). Autoradiograms and negatives from the Polaroid photographs of ethidium-stained gels were scanned, and the DNA was quantitated using a Molecular Dynamics densitometer with ImageQuant software (Molecular Dynamics, Sunnyvale, CA). In nonrestricted samples, forms conversion was followed by determining the concentration of any one form calculated as a fraction of the sum of all three forms. In restricted samples, the length of DNA fragments (determined by comparison to sized marker fragments of SV40) was used to determine the distance of the C-1027-induced break from the unique enzyme restriction site.

Analysis of C-1027-Induced Damage to Uninfected BSC-1 Cell Genomic DNA by Pulsed-Field Gel Electrophoresis. Logarithmically growing BSC-1 cells (1.3×10^6 per 60 mm plate) radiolabeled for 48 h with [2-^{14}C]thymidine (0.0125 μCi/mL) were rinsed once and incubated with 2.0 mL of non-radiolabeled medium for 30 min. C-1027 (0.1−100 nM) was added and incubation continued for 2 h. Except as noted, all manipulations after drug incubation were carried out at 4 °C. Plates were placed on ice and rinsed once with PBS. Cells were trypsinized for 3 min at 37 °C, washed once with PBS by centrifugation, and suspended in PBS at 2×10^7 cells/mL. The cell suspension was warmed for 2 min at 37 °C and mixed 1:1 with prewarmed 1% low gelling temperature agarose (Incert) in PBS. Agarose plugs were formed by pipeting 30 μL aliquots (3×10^5 cells) onto a Parafilm sheet placed on ice. If X-ray damage was being quantitated, non-C-1027-treated cells in plugs were X-ray-irradiated at the appropriate exposure. Agarose plus were removed to sterile 10 mL round-bottom plastic tubes containing 5 mL of 1% sarcosyl, 0.5 M EDTA, and 2 mg/mL proteinase K and incubated with gentle agitation for 20 h at 55 °C. Plugs were loaded into the wells of a 0.8% agarose gel, which were sealed with 0.5% low gelling temperature agarose. Pulsed-field gel electrophoresis using a Bio-Rad ChefDR II was carried out in TAE buffer for 89.8 h at 64 V with a 35 min pulse between field changes. Gels were soaked for 5 min in water and then transferred to a piece of Whatman filter paper and dried using a Bio-Rad gel slab dryer. The dried gel attached to the filter paper was covered with a 0.0005 in. Mylar sheet (Fralock, Canoga Park, CA) and placed in a phosphorimager cassette (Molecular Dynamics). After a 24 h exposure, the phosphorimage was scanned using a Molecular Dynamics Phosphorimager. The boundaries of the well hole were determined by viewing the phosphorimage using a color range (e.g., 10−100) that effectively reduced the background, thus eliminating all but the most intense signal. Each lane was scanned, and a drop line was marked on the scan at the position where the bottom of the well was located. DNA entering the well was quantitated from the drop line to the end of the lane, while well hole counts were quantitated from the signal located between the top and the bottom of the well. The intensity of the radioactive signal remaining in the well was expressed as a percent of total lane intensity.

SV40 DNA Accumulation in Virus-Infected BSC-1 Cells. BSC-1 cells were infected with SV40 virus as described earlier, and C-1027 was added 2 h later. After 4 h of drug treatment, cells were refed with fresh medium and incubation continued for an additional 36 h. Cells were lysed in SDS, digested with proteinase K, and analyzed for the presence of SV40 DNA by agarose gel electrophoresis. Forms I, II, and III were summed, and the drug-treated samples were expressed as a percent of control (0 drug) samples.

Incorporation of [^{3}H]Thymidine into Uninfected BSC-1 Cells. BSC-1 cells (5×10^5/35 mm plate) were treated with C-1027 in 2.0 mL of medium for 3 h at 37 °C, followed by the addition of 2 μCi/mL [^{3}H]thymidine and further incubation for 30 min. Cells were washed twice with PBS and divided into two aliquots. One aliquot was directly hydrolyzed in perchloric acid for 1 h at 70 °C to provide cpm uptake. The remainder was analyzed for acid insoluble radioactivity as described previously (Woynarowski & Konopa, 1981).

BSC-1 Cell Survival Assay. BSC-1 cell survival was assayed as described elsewhere with minor modifications (Zsido et al., 1991). Briefly, cells were seeded at 1.25×10^5 cells per 35 mm plate and grown for 48 h in MEM, yielding 5×10^5 cells per plate. Each plate was then refed with 1.0 mL of medium containing C-1027 at the appropriate concentration and incubated for 2 h at 37 °C. Following drug treatment, monolayers were washed twice with PBS and trypsinized. Samples were plated in duplicate at 10^2, 3×10^2, 10^3, 3×10^3, and 10^4 cells per 60 mm dish in 5 mL of MEM. After 10 days, colonies were stained with methylene blue and counted, and relative colony formation was calculated as a percent of colonies observed in control (non-drug-treated) culture plates.

RESULTS

SV40 DNA Topological Forms Conversion Induced by C-1027 in Infected BSC-1 Cells and in Purified DNA Preparations. Since C-1027 cytotoxicity has been correlated with the induction of intracellular (L1210) DNA strand damage (Sugimoto et al., 1990), we initially assayed the ability of this agent to damage the defined intracellular target, SV40 DNA. Damage to SV40 is readily measured by analyzing forms conversion of its supercoiled molecule. Conversion of supercoiled form I to nicked circular form II requires at least one nick per duplex DNA molecule, while at least two cuts per molecule are required for linearization to form III (Grimwade & Beerman, 1986). Forms are separated by agarose gel electrophoresis following treatment as described in the Experimental Procedures. Preliminary

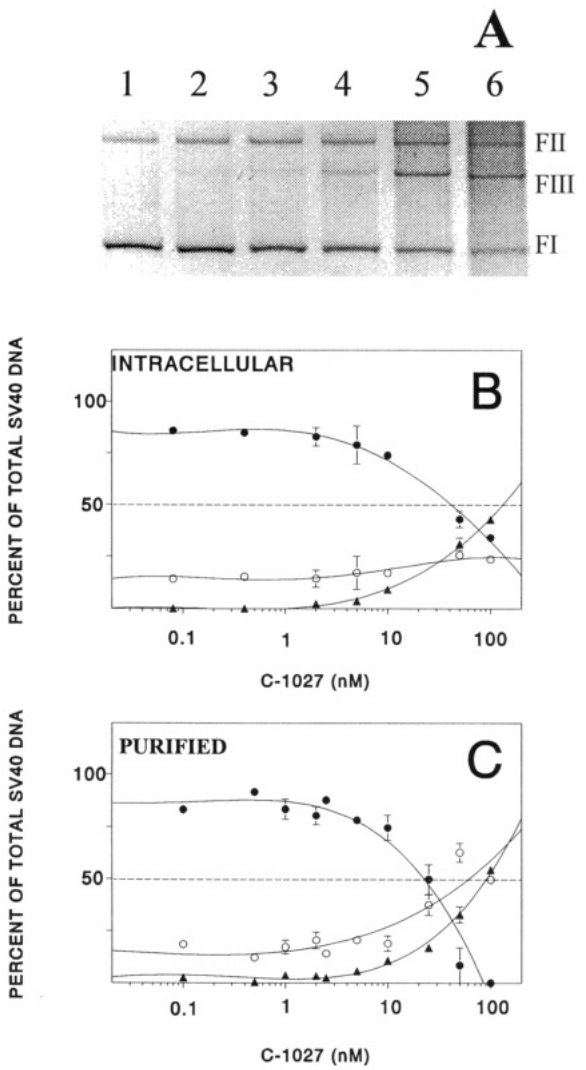

FIGURE 2: SV40 DNA forms conversion induced by C-1027 in infected BSC-1 cells and in purified DNA preparations. C-1027 treatment of SV40 DNA was as described in the Experimental Procedures. Drug-treated samples were subjected to electrophoresis on agarose gels and visualized by staining with ethidium bromide. Panel A: Densitometric scan of a Polaroid negative of a representative gel showing changes in intracellular SV40 form I, (FI), form II, (FII) and form III, (FIII) with C-1027 treatment at lanes (1) 0, (2) 2, (3) 5, (4) 10, (5) 50, and (6) 100 nM. Panel B: Graphic representation of forms conversion of intracellular SV40 with C-1027 concentrations of 0.08−100 nM. Panel C: Graphic representation of forms conversion of purified SV40 DNA upon treatment with 0.1−100 nM C-1027. In both panels B and C, the symbols correspond to FI (●), FII (○), and FIII (▲).

experiments found that maximal C-1027-induced damage to intracellular supercoiled SV40 DNA was achieved within 2 h after treatment, while a 15 min incubation with C-1027 was sufficient to produce maximal strand damage in purified SV40 DNA preparations. In addition, 1% SDS completely inhibited C-1027-induced SV40 DNA strand damage (data not shown). Thus, these conditions for the length of incubation and termination of the C-1027 reaction were used throughout the present study. A representative agarose gel showing C-1027-induced forms conversion of intracellular SV40 DNA is shown in Figure 2A. A gradual decrease in supercoiled form I accompanied by a substantial increase in form III was observed with C-1027 concentrations of 2−100 nM (lanes 2−6). By 50 nM (lane 5), form I was reduced by more than 50%. Only minor differences in the levels of form II were observed when the amount present in the control (lane 1) was compared to that in C-1027-treated samples. Thus, double-strand damage was a major result of C-1027 treatment of the intracellular supercoiled SV40 molecule.

From the AT-rich C-1027 cleavage site preference reported by others for purified DNA (Sugiura & Matsumoto, 1993; Xu et al., 1994), relatively random damage might be expected throughout the genome. However, the extreme cytotoxicity of C-1027 suggested that some characteristic of the cellular milieu might influence the ability of the drug to form lesions on intracellular DNA. For example, the incidence of single- or double-strand damage might differ between intracellular and purified DNA. Thus, a series of experiments was performed assaying, by forms conversion analysis, the extent of C-1027-induced damage to both intracellular and purified supercoiled SV40 DNA (Figure 2B and 2C, respectively). Figure 2B showed that the loss of intracellular form I was most pronounced between 10 and 100 nM C-1027, with a 50% decrease occurring at 40 nM drug. Similar to the intracellular data, damage to purified SV40 DNA was also most pronounced between 10 and 100 nM C-1027, with a 50% reduction in form I observed at 23 nM (Figure 2C). When drug concentrations were expressed as r values[1] (moles of drug/mole of nucleotide base pair) rather than as molarity, the amount of C-1027 necessary to effect forms conversion was lower for intracellular than for purified SV40 DNA (e.g., a 50% reduction in form I was achieved with C-1027 at $r = 0.002$ for intracellular and at $r = 0.0035$ for purified SV40 DNA). Thus, the intracellular environment (e.g., DNA conformation) did not inhibit, and may have enhanced to some extent, the ability of C-1027 to induce SV40 DNA strand damage. Interestingly, while an increase in intracellular form III was observed with C-1027 concentrations greater than 2 nM C-1027, the percent form II remained relatively stable (25−30% of total SV40 DNA) over the dose range tested. By contrast, when purified DNA was subjected to increasing concentrations of C-1027 up to 100 nM, the amount of form II increased, along with form III. Thus, C-1027 apparently induced both single- and double-strand damage to purified SV40, while progressive damage to intracellular SV40 was primarily double-stranded.

Site Specificity of C-1027 Double-Strand Damage to SV40 DNA. While the incidence of C-1027 double-strand damage differed when intracellular was compared to cell-free SV40 DNA, it was of interest to determine whether the location of these breaks was affected. To define regions where double-strand damage occurred, restriction enzyme digestion analysis, coupled with Southern blotting and hybridization to a ^{32}P-radiolabeled fragment of SV40 DNA, was performed with C-1027-treated intracellular or purified SV40 DNA. Figure 3A is a representative agarose gel showing the *Bgl*I restriction enzyme digestion pattern of C-1027-induced double-strand damage to purified (lanes 1−4) and intracellular (lanes 5−9) SV40 DNA. A distinct ladder of subbands was observed when purified SV40 DNA was treated with either 4 or 40 nM C-1027 (lanes 3 and 4, respectively), while some of the most prominent bands were visible with as little as 0.4 nM (lane 2). A similar pattern of subband formation was observed when intracellular SV40 DNA was treated with 10 and 50 nM C-1027 (lanes 8 and 9). After densitometric

[1] r values were calculated using a DNA concentration of 12 μg/35 mm plate for SV40-infected BSC-1 cells [see McHugh et al. (1994)].

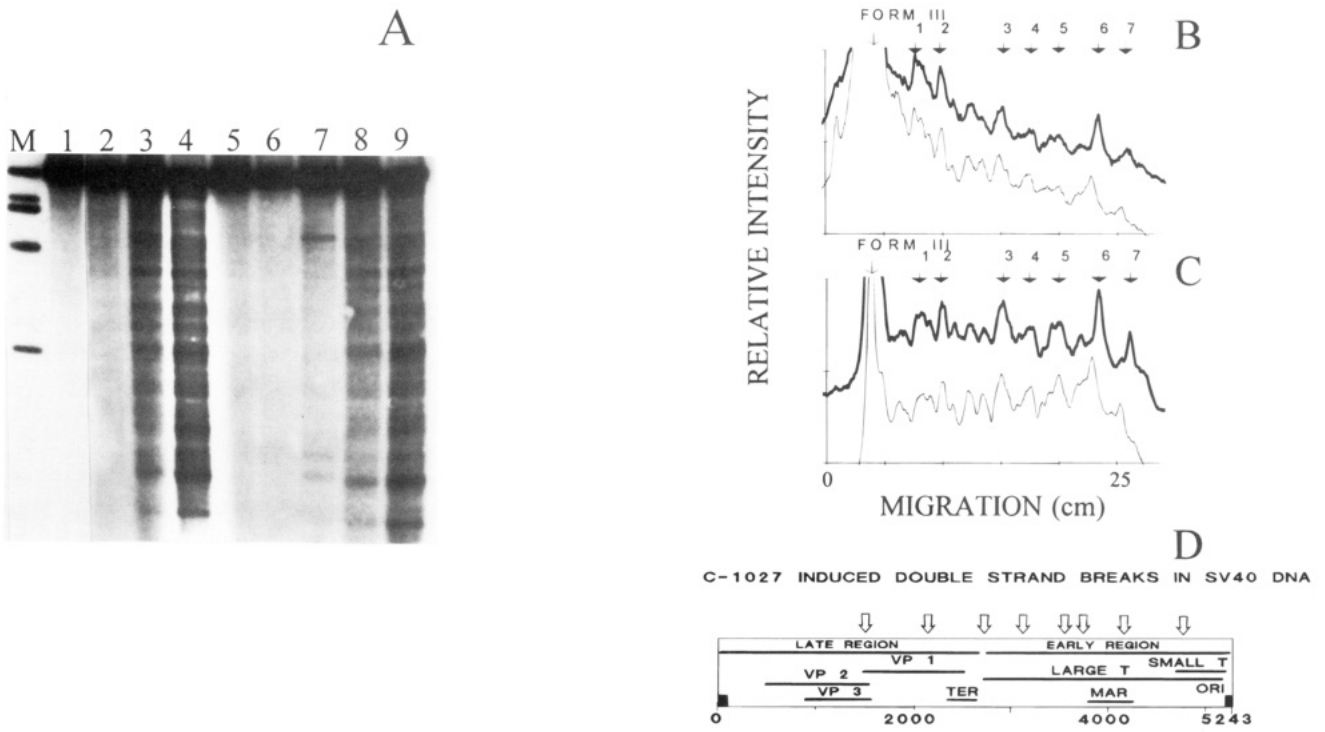

FIGURE 3: Site specificity of C-1027 double-strand damage to SV40 DNA. Intracellular and purified SV40 DNA were treated with C-1027 and digested with the single-cut restriction enzyme *Bgl*I as described in the Experimental Procedures. Panel A is a representative autoradiogram showing changes in the digestion pattern of purified (lanes 1−4) and intracellular (lanes 5−9) SV40 DNA with increasing concentrations of C-1027. M is an SV40 DNA size marker. Purified SV40 DNA was treated with (lane 1) 0, (2) 0.4, (3) 4, and (4) 40 nM C-1027. Intracellular DNA was treated with (lane 5) 0, (6) 0.4, (7) 2, (8) 10, and (9) 50 nM C-1027. Panels B and C show densitometric scans of selected lanes from the autoradiogram in panel A. Intracellular SV40 DNA is represented by the heavy lines and purified SV40 DNA by the lighter lines. Panel B shows low-dose C-1027 treatment of purified DNA at 4 nM (lane 3) and of intracellular SV40 at 10 nM (lane 8), while panel C shows high-dose C-1027 treatment of purified DNA at 40 nM and of intracellular SV40 at 50 nM (lanes 4 and 9, respectively). Numbers 1−7 on the graph indicate regions where C-1027 damage was observed and correspond to (1) 1500, (2) 2100, (3) 3200, (4) 3500, (5) 3900, (6) 4200, and (7) 4800 base pairs on the SV40 genome (the origin of replication is at 0 base pairs). Panel D is a simple map of the 5243 base pair SV40 genome. Regions where C-1027-induced intracellular damage occurs are indicated by the arrows. Coding sequences for large and small T-antigens, as well as a matrix-associated region (MAR), are located within the early region. Viral proteins 1, 2, and 3 (VP1, VP2, and VP3) are coded within the late region. TER and ORI refer to the terminus and the origin of SV40 DNA replication, respectively.

scanning of the autoradiogram, the data were expressed graphically for both low and high concentrations of C-1027 (Figure 3B and 3C, respectively). The heavy lines in parts B and C represent the treatment of intracellular SV40 DNA with 10 and 50 nM C-1027 ($r = 0.5 \times 10^{-3}$ and 2.5×10^{-3}), while lighter lines show the treatment of purified DNA with 4 and 40 nM C-1027 ($r = 0.2 \times 10^{-3}$ or 2×10^{-3}), respectively. Thus, the concentrations shown represent similar r values for C-1027 treatment of purified and intracellular DNA. A striking identity between intracellular and purified DNA-damaged regions is apparent even at low C-1027 concentrations (see panel B), with double-strand damage occurring at a number of specific sites throughout the genome. The location of seven of the most prominent sites are indicated by the numbered arrows: (1) 1500; (2) 2100; (3) 3200; (4) 3500; (5) 3900; (6) 4200; and (7) 4800. An additional damage site, between peaks 2 and 3 (around 2700 bp), which resolved into two bands at higher drug levels, was also identified. In general, other than an increase in subband intensity, little difference in site-directed DNA damage was observed at higher concentrations of C-1027 (see Figure 3C). Thus, C-1027 double-strand damage to both purified and intracellular SV40 DNA occurred nonrandomly and within the same regions of the genome. While no difference was observed in site preference between intracellular and purified DNA, a more precise analysis (e.g., at the level of nucleotide sequencing) would be required to eliminate the possibility of an effect of the cellular milieu on C-1027 cleavage sites.

The location of the C-1027 cut sites in relation to functional regions of the SV40 genome (Tooze, 1980) is shown in Figure 3D. The arrows indicate the regions targeted by C-1027 for double-strand damage. As can be seen, the majority of the cut sites are located in the early region of the genome, with significant damage observed throughout the coding region for large T-antigen [e.g., within the nuclear matrix-associated region (MAR) of SV40 (Pommier et al., 1990)]. Damage was also localized within the coding regions for the viral capsid proteins VP1, -2, and -3.

Quantitation of C-1027-Induced Intracellular SV40 DNA Single- and Double-Strand Damage. Previous reports detailed the induction of both single- and double-strand breaks by C-1027 in an extracellular environment (Xu et al., 1990; Sugiura & Matsumoto, 1993). However, a very recent study suggested that C-1027-induced single-strand breaks do not occur randomly, but are directed to sites in close proximity on opposite strands, leading to preferential formation of double- rather than single-strand breaks (Xu et al., 1994). Whether double-strand damage is a characteristic of intracellular C-1027 activity was examined using the data from Figure 2B to calculate single- and double-strand breaks in SV40 DNA according to the method of Cullinan et al. (1991)

Table 1: C-1027 Concentration-Dependent DNA Damage in BSC-1 Cells[a]

C-1027 r ($\times 10^{-4}$)	intracellular SV40			uninfected BSC-1 cell DNA
	DSB/10^6 NT[b]	SSB/10^6 NT	DSB/SSB	DSB/10^6 NT
1	2.4	7	0.34	0.027
10	16.2	29	0.53	0.27
40	40	54.8	0.73	0.90

[a] Double-strand (DSB) and single-strand (SSB) breaks in SV40 DNA were determined at the r values shown from the data in Figure 2B by dividing the fractional increase in form III (0.025, 0.17, and 0.42) or the fractional decrease in form I (0.073, 0.304, and 0.575), respectively, by the number of SV40 nucleotides (10, 486), according to the method of Cullinan et al. (1991). By using the rad equivalent damage (1000, 10 000, and 34 000) determined from the data shown in Figure 4C, C-1027-induced DSB in uninfected BSC-1 cell genomic DNA were calculated by the method of Ager et al. (1990),[3] who estimated the occurrence of 8.3×10^{-14} double-strand breaks per Dalton per rad. [b] NT, nucleotides.

(see Table 1). Even at the lowest r value (1×10^{-4}), which effected a less than 8% loss in form I, the incidence of double-strand breaks in (DSB) in SV40 intracellular DNA was high, with one double-strand lesion observed for every three single-strand breaks (SSB) (DSB/SSB = 0.34). At this level of form I conversion, Poisson distribution analysis predicts that a double-strand break is likely to result from two single-strand breaks located nearby on opposite strands, rather than from an accumulation of single-strand damage. With increasing drug dose, the ratio of double- to single-strand breaks continued to increase. For example, at C-1027 $r = 40 \times 10^{-4}$, corresponding to a 57% loss in form I, 73% of the single-strand breaks observed were associated with double-strand damage. Although some of these double-strand breaks probably result from the accumulation of single-strand breaks rather than double-strand cleavage across the DNA strand, double-strand damage appears to be an important component of C-1027 intracellular activity.

Pulsed-Field Gel Electrophoretic Analysis of DNA Damage Induced in Uninfected BSC-1 Cells. Having defined C-1027 reactivity with a discrete viral DNA target, we were interested in examining drug effects on genomic DNA from "normal" uninfected cells. The extent of C-1027 DNA damage was quantitated in uninfected BSC-1 cells using pulsed-field gel electrophoresis, as described in the Experimental Procedures. Figure 4A is a representative phosphorimage of BSC-1 cells treated with increasing C-1027. As described elsewhere by others, the amount of DNA remaining in the well hole after pulsed-field gel electrophoresis may be used to quantitate the extent of DNA double-strand damage (Ager et al., 1990). In the control (lane 1), the majority of the ^{14}C-radiolabel remained within the well hole. However, increased migration of ^{14}C-radiolabeled DNA into the gel was apparent even at the lowest C-1027 concentration tested (0.1 nM). With 25 nM (lane 6), most of the radioactivity had entered the gel, suggesting that extensive damage to genomic DNA had occurred. To compare the extent of damage induced by C-1027 with a known DNA-damaging agent, untreated BSC-1 cells embedded in agarose plugs were subjected to X-ray-irradiation prior to proteinase K digestion. Lanes 7 and 8 contain DNA from cells X-ray-irradiated with 1200 and 12 000 rad, respectively. DNA migration into the gel equivalent to that produced by 12 000 rad (see lane 8) was obtained with between 12.5 and 25 nM C-1027 (lanes 5 and 6, respectively).

Figure 4B is a graphic representation of data from a series of pulsed-field gels showing that the fraction of ^{14}C-radiolabeled DNA remaining in the well decreased as the X-ray dose increased. In control samples (no drug or X-ray treatment), the amount of DNA remaining in the well was typically 85−95% of the total, and some loss was detectable with as little as 400 rad. Roughly 3000 rad was sufficient to effect a 50% loss of DNA from the well.

Figure 4C shows the rad equivalent damage induced with increasing C-1027, estimated by comparing the loss of DNA from the well in C-1027-treated samples with that observed after X-ray irradiation (see Figure 4B). An increase in rad equivalent damage was observed above 0.1 nM C-1027 ($r > 4.3 \times 10^{-6}$).[2] By 100 nM C-1027 ($r = 4.3 \times 10^{-3}$), the damage induced in BSC-1 cell genomic DNA was equivalent to 37 000 rad. Nucleoid sedimentation analysis (Collins et al., 1989; Jackson et al., 1989), which can detect either single- or double-strand breaks, was also utilized for the analysis of C-1027-induced DNA damage. The range for DNA damage detection using this method was similar to that for pulsed-field gel electrophoretic analysis [i.e., changes in sedimentation were observed with C-1027 as low as $r = 6 \times 10^{-6}$ (data not shown)].

Comparison of C-1027 Concentration-Dependent DNA Damage in Uninfected and SV40-Infected BSC-1 Cells. The ability of C-1027 to induce strand damage in intracellular SV40 and genomic BSC-1 DNA is summarized in Table 1. Since drug incubation conditions for damage induction with uninfected BSC-1 cells and SV40-infected cells differed with respect to the number of cells per drug molecule (see Experimental procedures), it was not appropriate to use C-1027 molarity to compare damage in these two systems. Rather, the C-1027 concentration was expressed in terms of r values. Strand damage to uninfected BSC-1 cell genomic DNA was less frequent than to SV40 DNA. When uninfected BSC-1 cells were treated with C-1027 at $r = 1 \times 10^{-4}$, 0.027 double-strand breaks per 10^6 nucleotides (1000 rad equiv) were detected, more than 80-fold less than was observed for SV40. Even at the highest C-1027 level ($r = 40 \times 10^{-4}$), double-strand damage to SV40 was at least 40-fold greater than that determined for BSC-1 genomic DNA.

C-1027 Effects on DNA Synthesis. To evaluate the functional consequences of C-1027−DNA reactivity, drug effects on the synthesis of SV40 and uninfected BSC-1 cell genomic DNA were determined. The accumulation of SV40 DNA provided a measure of C-1027 effects on intracellular SV40 DNA synthesis (see Figure 5). Significant amounts of SV40 DNA were synthesized in the absence of drug. Increasing C-1027 concentrations reduced this accumulation, with 50% inhibition observed at 1.1 nM. C-1027 was a much more potent inhibitor of SV40 DNA accumulation in BSC-1 cells than was the related enediyne neocarzinostatin. Approximately 100 times more neocarzinostatin than C-1027 was required to inhibit SV40 synthesis by 50%.

C-1027 effects on genomic DNA synthesis were assayed by measuring the incorporation of [^{3}H]thymidine into uninfected BSC-1 cells (see Figure 6). Decreased [^{3}H]thymidine

[2] r values were calculated using a DNA concentration of 8.7 μg/10^6 uninfected BSC-1 cells.

[3] By using a molecular mass of 320 Da per nucleotide, DSB per 10^6 nucleotides (NT) was calculated by multiplying the rad equivalent damage by (8.3×10^{-14} DSB/Da/rad) × (320 Da) × (10^6 NT).

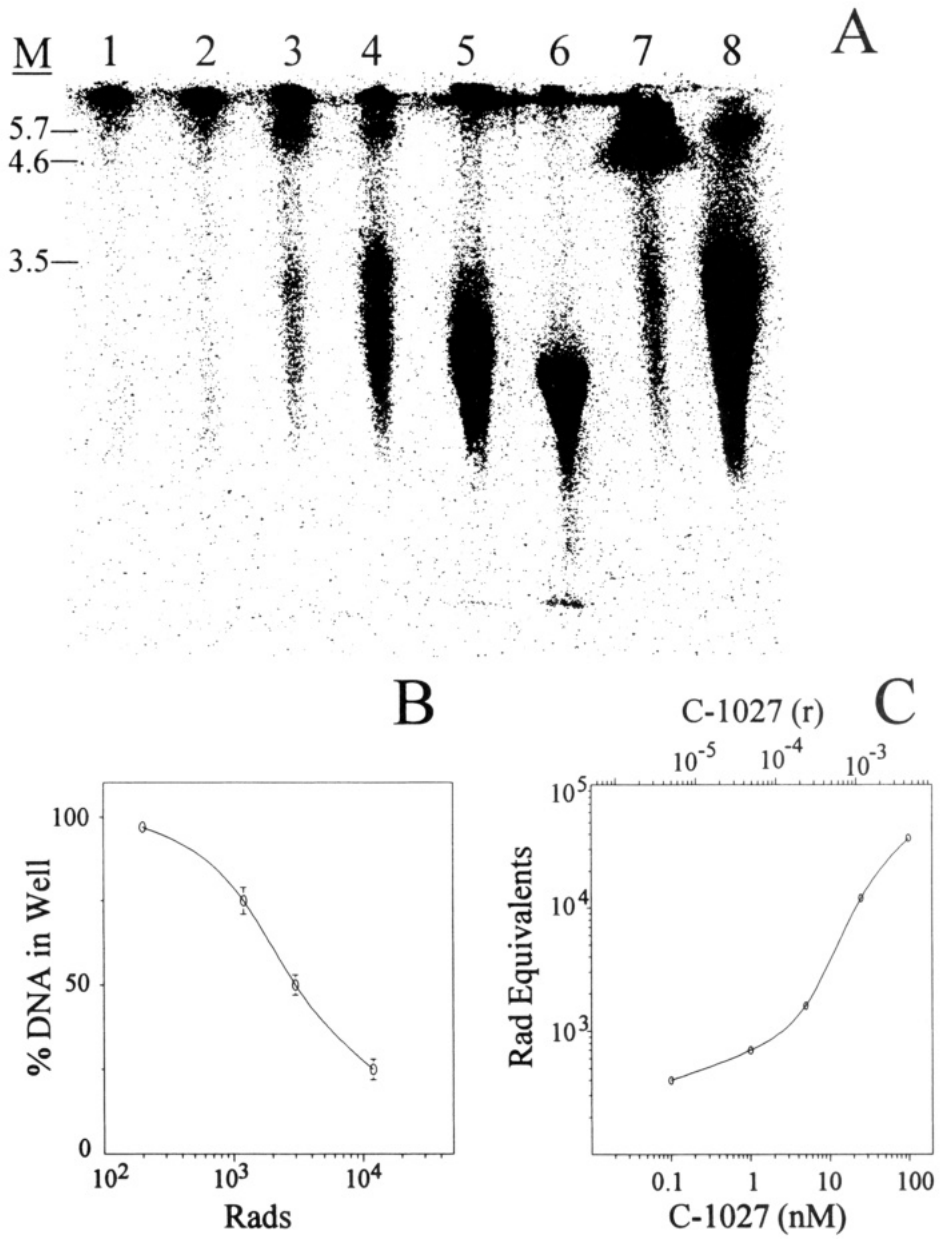

FIGURE 4: Pulsed-field gel electrophoretic analysis of C-1027 DNA damage induced in uninfected BSC-1 cells. ^{14}C-radiolabeled BSC-1 cells were treated with C-1027 and subjected to pulsed-field gel electrophoresis as described in the Experimental Procedures. Panel A is a representative phosphorimage obtained after exposure of the dried gel for 24 h, showing increased migration of DNA into the gel with increasing C-1027. Lanes 1−6 contain DNA from BSC-1 cells treated with (1) 0, (2) 0.1, (3) 1, (4) 5, (5) 12.5, and (6) 25 nM C-1027 (r = 0, 4.3×10^{-6}, 4.3×10^{-5}, 2.2×10^{-4}, 5.4×10^{-4}, and 1.1×10^{-3}, respectively). Lanes 7 and 8 contain DNA from BSC-1 cells embedded in agarose plus and irradiated with 1200 and 12 000 rad, respectively. M shows the position of *S. pombe* size markers (in megabases). Panel B: Graphic representation of the amount of DNA remaining in the well after electrophoresis of ^{14}C-radiolabeled DNA from X-ray-irradiated BSC-1 cells. The radioactivity per lane was summed and the amount remaining in the well was expressed as a percent of the total radioactivity. Panel C: rad equivalent damage induced with increasing C-1027. rad equivalent damage was estimated by comparing the loss of DNA from the well in C-1027-treated samples with that observed after X-ray irradiation (see panel B).

incorporation was noted above 0.01 nM C-1027, with a decrease of more than 80% observed at 0.1 nM. The effect of C-1027 on [^{3}H]thymidine incorporation was accompanied by inhibition of the uptake of the radiolabeled precursor. However, the reduction in the radiolabeled pool of thymidine nucleotides was significantly less than the inhibition of precursor incorporation into DNA. For example, a 50% inhibition of uptake required at least 20-fold more C-1027 (0.4 nM) than did a similar reduction in incorporation (0.02 nM). Interestingly, a 50% reduction in SV40 accumulation required 1.1 nM C-1027 (see Figure 5). Thus, C-1027-induced DNA synthesis inhibition was more pronounced in uninfected than in SV40-infected cells.

As with SV40 DNA accumulation, C-1027 and neocarzinostatin effects on the incorporation of [^{3}H]thymidine into genomic DNA were compared. Neocarzinostatin inhibited [^{3}H]thymidine incorporation at higher concentrations than did C-1027 (e.g., a 50% reduction in incorporation was observed with 65 nM neocarzinostatin). Some reduction in uptake, as well as incorporation, of [^{3}H]thymidine was also observed with neocarzinostatin treatment of BSC-1 cells.

C-1027 Effects on Relative Colony Formation. A unique aspect of C-1027 activity is its extreme cytotoxicity, with effective concentrations as low as 10^{-5} pM reported with certain tumor cell lines in culture (Zhen et al., 1989). Figure 7 shows the effect of increasing C-1027 on BSC-1 cell colony

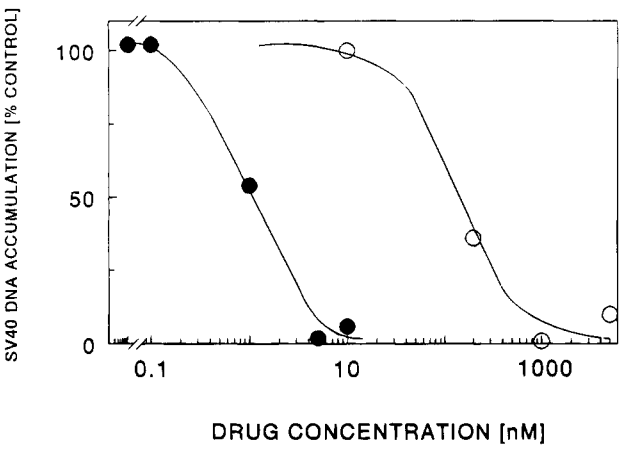

FIGURE 5: Inhibition of SV40 DNA accumulation in virus-infected BSC-1 cells. SV40 DNA accumulation in infected BSC-1 cells was assayed as described in the Experimental Procedures. Forms I, II, and III were summed, and the drug-treated samples were plotted as a percent of control (0 drug) samples ± SEM. Cells were treated with either C-1027 (●) or neocarzinostatin (○).

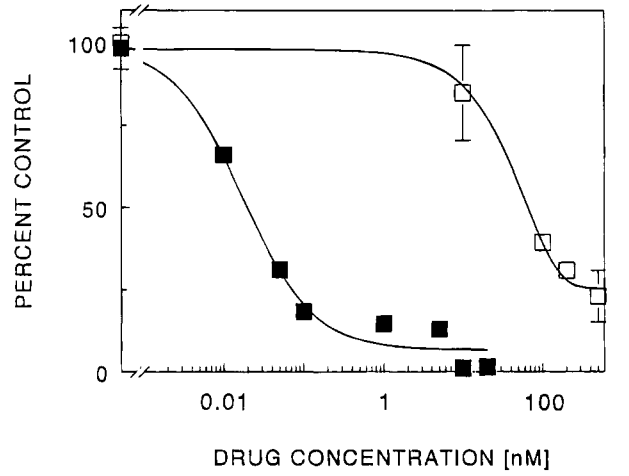

FIGURE 6: Inhibition of [^{3}H]thymidine incorporation in uninfected BSC-1 cells. Incorporation of [^{3}H]thymidine was performed as described in the Experimental Procedures. Incorporation was expressed as a percent of control (no drug) samples and was plotted ± SEM. Cells were treated with either C-1027 (■) or neocarzinostatin (□).

formation. Colony formation was a more sensitive measure of C-1027 activity than either pulsed-field detection of DNA damage or incorporation of [^{3}H]thymidine (see Figures 4C and 6), with effects observed as low as 10^{-2} pM. With 0.3 and 14 pM, colony formation was reduced by 50% (D_{50}) and 90% (D_{10}), respectively.

DISCUSSION

C-1027 is the most potent of the enediyne compounds described to date, with respect to both DNA-damaging activity and cytotoxicity (Zhen et al., 1989; Xu et al., 1990; Sugiura & Matsumoto, 1993). The activity of C-1027 resides in its chromophore, consisting of a nine-membered enediyne ring, which is structurally related to both the neocarzinostatin and kedarcidin chromophores (Yoshida et al., 1993). While the latter agents, as well as other enediyne structures (e.g., esperamicins, calicheamicins, and dynemicins), require a triggering mechanism to initiate activation of the enediyne (e.g., thiols), C-1027 requires only room temperature for

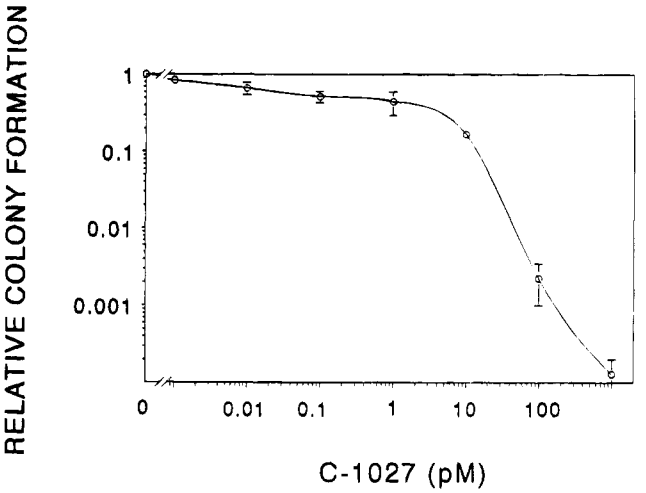

FIGURE 7: C-1027 effects on relative colony formation by uninfected BSC-1 cells. The assay for relative colony formation in the presence of increasing doses of C-1027 was performed as described in the Experimental Procedures. Data are plotted ± SEM.

activation (Zhen et al., 1989; Sugiura & Matsumoto, 1993). This lack of a requirement for an extraneous trigger to initiate C-1027 activity is a possible explanation for its extremely potent DNA reactivity relative to other enediyne agents. Another member of the protein–chromophore class of antibiotics, auromomycin (formerly known as macromomycin), also does not require sulfhydryl for activation (Beerman, 1979). Like C-1027, auromomycin is extremely cytotoxic, with effects observed as low as 10^{-11} M (Rauscher et al., 1990).

The intracellular environment did not reduce the ability of C-1027 to damage SV40 DNA. C-1027 damage to uninfected BSC-1 intracellular DNA also was relatively unaffected by the cellular milieu (data not shown).[4] By contrast, neocarzinostatin-induced strand damage was less pronounced in intact cells than in purified DNA preparations by a factor of 200 or 14 000, when either 935.1 cell episome or SV40, respectively, was the DNA target (Grimwade & Beerman, 1986; Cobuzzi et al., 1994). This difference in intracellular potency between C-1027 and neocarzinostatin may be due to differences in uptake of the two drugs. For example, while aminopeptidase activity has been associated with the C-1027 holoantibiotic (Sakata et al., 1992), endoprotease activity capable of digesting histones (e.g., histone H1) is reportedly associated with the neocarzinostatin apoprotein (Zein et al., 1993). It is postulated that aminopeptidase activity, by interaction with cell-surface proteins, may facilitate the entry of C-1027 into cells. However, rather than enhancing drug entry into the cell, the neocarzinostatin protease may facilitate the delivery of the chromophore to the target DNA by the removal of histones from nuclear chromatin. Aminopeptidase activity has also been found associated with the highly cytotoxic auromomycin holoantibiotic (Zaheer et al., 1985).

Although the amount of C-1027 required to induce single-strand damage in SV40 DNA was similar in purified and intracellular assays, double-strand damage (i.e., accumulation of form III) was more pronounced with intracellular treat-

[4] Cells were embedded in agarose and treated with C-1027 either before or after digestion with proteinase K to remove chromatin proteins, and rad equivalent damage was detected by pulsed-field gel electrophoresis.

ment. A detailed study of rate constants currently underway further indicates that C-1027 induces more double-strand breaks on intracellular DNA than on its extracellular component (Dabrowiak et al., unpublished observation). Characteristics of both the enendiyne−protein molecule and the DNA target may play a role in this enhanced intracellular double-strand damage. While both purified DNA and intact cells are treated with the C-1027 holoantibiotic, intracellular DNA is likely to interact with the chromophore alone, rather than with the noncovalent chromophore−protein complex (Sakata et al., 1992). Thus, intracellular binding site specificity is directed by the chromophore. By contrast, purified DNA is exposed to the C-1027 holoantibiotic, and chromophore binding is dependent to some extent on the tertiary structure of the apoprotein moiety (Matsumoto et al., 1993). Qualitative differences between purified and intracellular SV40 DNA may also limit strand damage. For example, while purified SV40 DNA exists as a supercoiled molecule, lytically infected BSC-1 cells contain rapidly replicating SV40 DNA. SV40 replicative intermediates exhibit varying degrees of superhelicity (Tooze, 1980) and may promote the formation of double-strand breaks by reducing the distance between preferred binding sequences on opposite strands. A recent report described a role for chromatin proteins in the effective formation of enediyne-induced intracellular double- rather than single-strand damage. Neocarzinostatin, which also effects enhanced formation of double-strand breaks in intracellular compared to purified SV40 DNA reactions (Grimwade & Beerman, 1986), was found to induce DNA sequence-specific abasic sites on one DNA strand (Kappen & Goldberg, 1989). In chromatin (but not in purified DNA preparations), these sites were rapidly converted to double-strand breaks, possibly by reaction with histone amines (Bennett et al., 1993).

While the double-strand break frequency was more pronounced in intact cells than in purified DNA, the formation of double-strand breaks in SV40 was noted under both sets of conditions. A mechanism for C-1027 double-strand break induction in purified DNA was postulated recently by others (Xu et al., 1994). Using plasmid (pBR322) DNA, double-strand damage was localized to specific AT-rich sequences and defined as cleavage adjacent to an adenine on one strand and either an adenine or a thymine on the opposite strand, two nucleotide bases apart. The authors suggested that single-strand breaks that were not associated with double-strand lesions occurred by an alternate DNA binding mode. Whether this mechanism is relevant to intracellular C-1027−DNA interactions has not been determined.

Examination of C-1027-induced double-strand damage with both cell-free and intracellular SV40 revealed identical regions of nonrandom damage located throughout the 5243 base pair genome. In view of the reported AT-rich sequence specificity of C-1027-induced DNA damage, it was not surprising that the regions with the most intense damage were AT-rich relative to the whole genome. For example, the sequence of the entire SV40 genome is 60% AT and 40% GC (GenBank). In contrast, the region around 4200 (4150−4250) that showed intense damage was 69% AT. Thus, damage occurring at specific coding sequences (see Figure 3D) likely is due to the presence of AT-rich sites rather than to any specific targeting of the gene itself. An earlier report from this laboratory described the SV40 DNA cleavage site preference for neocarzinostatin and a related agent, auromomycin (Grimwade et al., 1988). As with C-1027, the double-strand site preference for each of these agents was the same, regardless of whether cell-free or chromatin DNA was used. This suggested that damage was directed by the sequence rather than by any conformational alterations induced by chromatin association or compaction. In addition, while a large number of double-strand damage sites were observed throughout the SV40 genome, both neocarzinostatin and auromomycin showed a preference for regions around 4000 (within the MAR region) and 3200 base pairs, respectively, which were among the sites subject to C-1027 damage induction.

A consequence of C-1027 treatment is the inhibition of DNA replication in eukaryotic cells (Sugimoto et al., 1990; Xu et al., 1990). In the present study, when BSC-1 cells were treated with C-1027 shortly after SV40 infection, a potent inhibition of the accumulation of viral DNA was observed. Such inhibition of SV40 DNA synthetic processes might well be predicted from the intensity of the double-strand damage induced by C-1027 within the coding region for large T-antigen, a protein essential for the initiation of SV40 viral DNA synthesis (Tooze, 1980). Also of possible importance is the damage observed around 4200 base pairs, within the nuclear matrix-associated region (MAR) of SV40 DNA (Pommier et al., 1990). The nuclear matrix reportedly plays a pivotal role in DNA replication [for a review, see Fernandes and Catapano (1991)]. Thus, damage to the MAR region or to other portions of the coding region for large T-antigen would be expected to reduce the rate of SV40 viral DNA synthesis. The profile of site-specific damage induced by C-1027 strongly resembled that reported earlier with the DNA-alkylating agent, CC-1065 (McHugh et al., 1994). CC-1065-induced apparent double-strand lesions also resulted in damage within the early region of SV40 DNA, specifically around 4200. Although these agents differ in their mechanisms of interaction with DNA, their reactivity within the same regions of the SV40 genome probably relates to the fact that CC-1065 (Bhuyan et al., 1982), as well as C-1027, reacts with the minor groove preferentially at AT-rich regions.

A selective effect was observed when C-1027-induced damage to SV40 DNA in lytically infected cells was compared to damage in uninfected BSC-1 cell DNA. When cells were treated with C-1027 r values from 1×10^{-4} to 40×10^{-4}, double-strand breaks were from 80- to 40-fold more frequent in SV40 than in BSC-1 cell genomic DNA (see Table 1). SV40 also was more sensitive to C-1027-induced strand damage (by a factor of 2) than was a supercoiled, episomal DNA target in uninfected murine 935.1 cells [see Cobuzzi et al. (1994)].[5] Increased damage to viral DNA compared to DNA in normal, uninfected cells may be due simply to disruptions at the cell surface of virally transformed cells. These include changes in the permeability of nuclear and plasma membranes, which permit increased transport of agents across the cell membrane (Tooze, 1980). Such changes have been described during the later stages of SV40 viral infection (i.e., during or after the process of viral encapsidation) and should be underway by 40 h postinfection, the time at which infected cells were treated with C-1027 in

[5] A 50% reduction in supercoiled form I SV40 or episomal DNA was achieved with C-1027 $r = 2.5 \times 10^{-3}$ or $r = 5 \times 10^{-3}$, respectively.

the DNA damage assays described herein.

By contrast, inhibition of DNA synthesis was much more pronounced in uninfected than in SV40-infected BSC-1 cells. This observation may reflect increased repair of the SV40 genome in infected cells compared to uninfected BSC-1 cell DNA. Repair reportedly occurs selectively in rapidly transcribing genes (Bohr, 1987; Deng & Nickoloff, 1994). Transcribed sequences comprise less than 1% of the genome of normal cells (Bohr, 1987), compared to 50% of the SV40 genome in lytically infected cells (Kelly & Nathans, 1977). Thus, repair of C-1027-induced lesions in SV40 DNA may be enhanced relative to that in uninfected BSC-1 cell genomic DNA.

C-1027 cytotoxicity was observed at much lower levels (10^{-2} pM) than those required for the detection of either DNA damage or DNA synthesis inhibition in uninfected BSC-1 cells. Likewise, earlier studies have reported C-1027-induced cytotoxicity with concentrations as low as 10^{-5} pM (Zhen et al., 1989). While rapid induction of single- and double-strand damage has been reported to correlate with cytotoxicity (Sugiura & Matsumoto, 1993), drug-induced programmed cell death (i.e., apoptosis) cannot be ruled out. Indeed, apoptosis was reported elsewhere as a mechanism for cell death induced by certain synthetic dynemicin-like enediyne structures (Nicolaou et al., 1993b). By contrast, intact dynemicin analogs did not appear to exert their activity via activation of programmed cell death. Further studies are necessary to define precisely the role of apoptosis in C-1027 activity.

In conclusion, C-1027 is a potent inducer of double-strand breaks in intracellular DNA targets. Regions of the SV40 genome associated with attachment to the nuclear matrix and synthesis of early viral proteins contain AT-rich sequences and are preferentially targeted by C-1027. A greater frequency of C-1027-induced double-strand damage was noted in intracellular SV40 than in BSC-1 cell DNA. Functional consequences of C-1027 treatment include decreased DNA synthesis in both uninfected and SV40-infected BSC-1 cells, as well as potent cytotoxicity. Future studies will use two-dimensional gel electrophoresis to assess the effects of C-1027-induced damage at these AT-rich functional regions on specific steps in the process of SV40 DNA replication.

REFERENCES

Ager, D. D., Dewey, W. C., Gardiner, K., Harvey, W., Johnson, R. T., & Waldren, C. A. (1990) *Radiat. Res. 122*, 181−187.

Beerman, T. A. (1979) *Biochim. Biophys. Acta 564*, 361−371.

Bennett, R., Swerdlow, P. S., & Povirk, L. F. (1993) *Biochemistry 32*, 3188−3195.

Bhuyan, B. K., Newell, K. A., Crampton, S. L., & Von Hoff, D. D. (1982) *Cancer Res. 42*, 3532−3537.

Bohr, V. A. (1987) *Dan. Med. Bull. 34*, 309−320.

Cobuzzi, R. J., Kotsopolous, S. K., Otani, T., & Beerman, T. A. (1994) *Biochemistry* (in press).

Collins, J. M., Wood, S. H., & Chu, A. K. (1989) *Biochim. Biophys. Acta 563*, 264−276.

Cullinan, E. B., Gawron, L. S., Rustum, Y. M., & Beerman, T. A. (1991) *Biochemistry 30*, 3055−3061.

Deng, W. P., & Nickoloff, J. A. (1994) *Mol. Cell. Biol. 14*, 391−399.

Fernandes, D. J., & Catapano, C. V. (1991) *Cancer Cells 3*, 134−140.

Goldberg, I. H., Hatayama, T., Kappen, L. S., Napier, M. A., & Povirk, L. F. (1981) in *Molecular Actions and Targets for Cancer Chemotherapeutic Agents* (Sartorelli, A. C., Ed.) pp 163−191, Academic Press, New York.

Grimwade, J., & Beerman, T. A. (1986) *Mol. Pharmacol. 30*, 358−363.

Grimwade, J. E., Cason, E. B. & Beerman, T. A. (1987) *Nucleic Acids Res. 15*, 6315−6329.

Grimwade, J., Cullinan, E. B. & Beerman, T. A. (1988) *Biochim. Biophys. Acta 950*, 102−112.

Hu, J., Xue, Y.-C., Xie, M.-Y., Zhang, R., Otani, T., Minami, Y., Yamada, Y., & Marunaka, T. (1988) *J. Antibiot. 41*, 1575−1579.

Jackson, D. A., Pearson, C. K., Fraser, D. C., Prise, K. M., & Wong, S. Y. (1989) *J. Cell Sci. 92*, 37−49.

Kappen, L. S., & Goldberg, I. H. (1989) *Biochemistry 28*, 1027−1032.

Kelly, T. J., Jr., & Nathans, D. (1977) *Adv. Virus Res. 21*, 85−173.

Matsumoto, T., Okuno, Y., & Sugiura, Y. (1993) *Biochem. Biophys. Res. Commun. 195*, 659−666.

McHugh, M. M., Woynarowski, J. M., Mitchell, M. A., Gawron, L. S., Weiland, K. L., & Beerman, T. A. (1994) *Biochemistry 33*, 9158−9168.

Myers, A. G., Proteau, P. J., & Handel, T. M. (1988) *J. Am. Chem. Soc. 110*, 7212−7214.

Nicolaou, K. C., Dai, W.-M., Tsay, S.-C., Estevez, V. A., & Wrasidlo, W. (1992) *Science 256*, 1172−1178.

Nicolaou, K. C., Smith, A. L., & Yue, E. W. (1993a) *Proc. Natl. Acad. Sci. U.S.A. 90*, 5881−5888.

Nicolaou, K. C., Stabila, P., Esmadli-Azad,B., Wrasidlo, W., & Hiatt, A. (1993b) *Proc. Natl. Acad. Sci. U.S.A. 90*, 3142−3146.

Pommier, Y., Cockerill, P. N., Kohn, K. W., & Garrard, W. T. (1990) *J. Virol. 64*, 419−423.

Rauscher, F. J., III, Beerman, T. A., & Baker, R. M. (1990) *Mol. Pharmacol. 38*, 198−206.

Sakata, N., S.-Tsuchiya, K., Moriya, Y., Hayashi, H., Hori, M., Otani, T., Nagai, M., & Aoyagi, T. (1992) *J. Antibiot. 45*, 113−117.

Sambrook, J., Fritsch, E. F., & Maniatis, T. (1989) *Molecular Cloning: A Laboratory Manual*, Cold Spring Harbor Laboratory Press, Cold Spring Harbor, NY.

Sugimoto, Y., Otani, T., Oie, S., Wierzba, K., & Yamada, Y. (1990) *J. Antibiot. 43*, 417−421.

Sugiura, Y., & Matsumoto, T. (1993) *Biochemistry 32*, 5548−5553.

Tooze, J. (1980) *Molecular Biology of Tumor Viruses, pt. 2*, Cold Spring Harbor Laboratory Press, Cold Spring Harbor, NY.

Woynarowski, J. M., & Konopa, J. (1981) *Mol. Pharmacol. 19*, 97−102.

Xu, Y.-J., Li, D.-D., & Zhen, Y.-S. (1990) *Cancer Chemother. Pharmacol. 27*, 41−46.

Xu, Y.-J., Zhen, Y.-S., & Goldberg, I. H. (1994) *Biochemistry 33*, 5947−5954.

Yoshida, K.-I., Minami, Y., Azuma, R., Saeki, M., & Otani, T. (1993) *Tetrahedron Lett. 34*, 2637−2640.

Zaheer, A., Zaheer, S., & Montgomery, R. (1985) *J. Biol. Chem. 260*, 11787−11792.

Zein, N., Casazza, A. M., Doyle, T. W., Leet, J. E.,Schroeder, D. R., Solomon, W., & Nadler, S. G. (1993) *Proc. Natl. Acad. Sci. U.S.A. 90*, 8009−8012.

Zhen, Y.-S., Ming, X.-Y., Yu, B., Otani, T., Saito, H., & Yamada, Y. (1989) *J. Antibiot. 42*, 1294−1298.

Zsido, T. J., Woynarowski, J. M., Baker, R. M., Gawron, L. S., & Beerman, T. A. (1991) *Biochemistry 30*, 3733−3738.

BI9419792